JOURNAL OF MATERIALS SCIENCE 29 (1994) 2401–2405

Viscoelasticity of ceramics at high temperatures

H. PETERLIK
Institute of Solid State Physics, University of Vienna, Strudlhofg. 4, A-1090 Vienna, Austria

The dependence of the fracture toughness, K_{IC}, on the loading rate has been calculated. On the basis of linear elastic fracture mechanics (LEFM) a strong dependence of the fracture toughness on the loading rate is obtained if subcritical crack growth is taken into account. If the subcritical crack growth parameters n and B are sufficiently small, which correspond to a high velocity of crack extension, the fracture toughness should decrease at lower loading rates. This behaviour is similar to the well-known decrease of bending strength. The experimental results for alumina containing glassy phase as a model material, however, show a maximum in a certain regime of loading rates. A model is established, which combines LEFM and the viscoelasticity, and leads to a maximum of K_{IC} at a certain loading rate dependent on the viscosity of the glassy phase.

1. Introduction

The development of ceramics for application in technical systems, which have to sustain high temperatures, has been a field of extensive research for a long time. Ceramics are very promising materials because of their oxidation resistance, good mechanical properties at high temperatures and high specific strength.

Four-point bending tests are very common to determine the bending strength and the fracture toughness. According to linear elastic fracture mechanics (LEFM), the fracture toughness should be a material constant. At high temperatures, however, this is not the case. In the literature it is shown that ceramics with second phases have a strong dependence of the fracture toughness on the loading rate and/or the temperature, e.g. silicon nitride [1], alumina with glassy phase [2] and silicon-infiltrated silicon carbide [3]. Even the bending strength can rise by up to 40% at elevated temperatures (mullite-based ceramic [4]), where the energy dissipation by plastic relaxation of an intergranular silica-rich phase was proved to be responsible for this behaviour. Thus it is not surprising that a standardization procedure for the bending strength at high temperatures has been recently proposed [5, 6], and the standardization procedure for fracture toughness is still in discussion.

For alumina produced without sintering aids, it was shown that the fracture toughness is actually a constant [2]. Thus it was assumed that the second phase is responsible for the dependence on loading rate and temperature. In the present work, the dependence of the fracture toughness on the loading rate according to LEFM and due to a viscoelastic model have been compared. The viscoelastic model is able to describe the observed experimental behaviour of alumina with glassy phase. This material was used as a model material, because it shows the maximum in fracture toughness at moderate temperatures of 900 °C. However, the model should be valid for all ceramics containing sintering aids.

2. Fracture toughness dependence on loading rate in LEFM

The following two equations are well known in LEFM: the equation to compute the K-factor from four-point bending experiments is given by

$$K(t) = \sigma Y a^{1/2} = \frac{3eF(t)}{BW^2} Y a^{1/2} \quad (1)$$

where Y is a geometry-dependent function [7], e the lever arm, B and W the breadth and width of the specimen, and $F(t)$ the applied force. The crack velocity obeys a power law

$$\dot{a} = AK_I^n = \tilde{A}\left(\frac{K_I}{K_{IC}}\right)^n \quad (2)$$

Usually, the fracture toughness, K_{IC}, can be obtained from Equation 1 by measuring the maximum load, which a specimen with known crack length, a_0, (e.g. a sufficiently small cut by a diamond saw) is able to sustain.

This is only valid if the crack length, a_0, is large in comparison to the crack extension due to subcritical crack growth. If this is not the case, one can establish an equation for the K-factor, where the additional crack extension by subcritical crack growth is taken into account

$$K(t) = \frac{3eF(t)}{BW^2} Y[a(t)]^{1/2} = \frac{3eF(t)}{BW^2} Y\left[a_0 + \int_0^t d\tau\, \dot{a}(\tau)\right]^{1/2} \quad (3)$$

Inserting the power law (Equation 2) into Equation 3 results in an integral equation for the K-factor

$$K(t) = \frac{3eF(t)}{BW^2} Y\left\{a_0 + \int_0^t d\tau\, \tilde{A}\left[\frac{K(\tau)}{K_{IC}}\right]^n\right\}^{1/2} \quad (4)$$

For $F(t) = \dot{F}t$, a constant loading rate, Equation 4 can

be transformed into a differential equation by squaring and differentiating it with respect to time. The resulting differential equation is easy to solve, and one obtains for $n > 2$

$$K(t) = t^{n-2} \Big/ \left[\text{constant} - \frac{n-2}{2(n+1)} \left(\frac{3eYF\dot{}}{BW^2} \right)^2 \frac{\tilde{A}}{K_{IC}^n} t^{n+1} \right] \tag{5}$$

Now the K-factor has to meet the following conditions: it must be zero at the beginning and it must be equal to the fracture toughness K_{IC} at the moment of fracture, t_{wce}, where the index denotes *w*ith *c*rack *e*xtension:

$$K(0) = 0 \tag{6a}$$

$$K(t_{wce}) = K_{IC} \tag{6b}$$

Using the second condition, one can determine the constant

$$\text{constant} = \left(\frac{t_{wce}}{K_{IC}} \right)^{n-2} + \frac{n-2}{2(n+1)} \left(\frac{3eYF\dot{}}{BW^2} \right)^2 \frac{\tilde{A}}{K_{IC}^n} t_{wce}^{n+1} \tag{7}$$

By introducing the constant into Equation 5, the actual K-factor can be computed. The most interesting point, however, is Equation 7. If there is no subcritical crack growth, the second term on the right-hand side in Equation 7 vanishes, and Equation 7 thus is reduced to

$$\text{constant} = \left(\frac{t_{nce}}{K_{IC}} \right)^{n-2} \tag{8}$$

where the index denotes the time to fracture, when *n*o *c*rack *e*xtension is present. Using this term as the constant in Equation 7, one obtains an equation for the "real" fracture time, t_{wce}, in relation to the "usual" fracture time, t_{nce}, when no crack extension during the experiment is taken into account. Hence the relation of the two times is given by

$$t_{wce}^{n+1} \frac{K_{IC}^2}{t_{nce}^2 B Y^2 a_0 (n+1)} + t_{wce}^{n-2} = t_{nce}^{n-2} \tag{9}$$

where $B = 2K_{IC}^2/[\tilde{A}(n-2)Y^2]$, which is usually determined by measuring the bending strength at different loading rates. From Equation 9 one can compute the time to fracture from the starting crack length, a_0, and the subcritical crack extension parameters B and n. If there is subcritical crack growth, the fracture toughness, which is measured in the experiment, can therefore be considerably lower! The fracture times, t_{wce} and t_{nce}, refer directly to the fracture toughness with and without subcritical crack extension

$$K_{IC}^{wce} = \text{constant } \dot{F}\, t_{wce} \tag{10a}$$

$$K_{IC}^{nce} = \text{constant } \dot{F}\, t_{nce} \tag{10b}$$

The influence of a variation of the crack extension parameter B (50, 500 and 5000 MPa^{2}s) can be seen in Fig. 1. Decreasing B, i.e. higher crack velocity, leads to a shift of the values of $K_{IC}^{wce}/K_{IC}^{nce}$ to higher loading rates. In the diagram the dashed lines represent the time to fracture, which is common in fracture toughness experiments (1–10 s). The influence of different values of n is much stronger: Fig. 2 shows the ratio $K_{IC}^{wce}/K_{IC}^{nce}$ for $n = 10$, 20, 50 and 100 and $B = 500$ MPa^{2}s. At low loading rates, one observes that the fracture toughness decreases with the loading rate

$$K_{IC}(\dot{F}) \propto \dot{F}^{1/(n+1)} \tag{11}$$

This can be easily read off from Equation 9: for long times, the second term on the left-hand side can be neglected, because it is small in comparison to the first term. Then t_{wce}^{n+1}/t_{nce}^2 is proportional to t_{wce}^{n-2}. Thus it follows that $t_{wce} \propto t_{nce}^{n/n+1}$. The fracture time without subcritical crack growth is inversely proportional to the loading rate: $t_{nce} \propto \dot{F}^{-1}$. Now the measured fracture toughness is

$$K_{IC}^{wce} = \text{constant } \dot{F}\, t_{wce} \propto \dot{F}\dot{F}^{-\frac{n}{n+1}} = \dot{F}^{\frac{1}{n+1}} \tag{12}$$

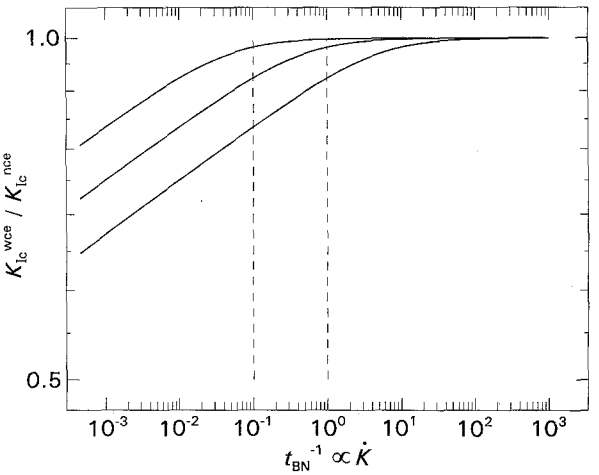

Figure 1 Influence of different values of the crack extension parameter, B, on fracture toughness in the LEFM theory: $B = 50$, 500, 5000 MPa^{2}s, $n = 20$. (– – –) The usual time range of fracture toughness experiments.

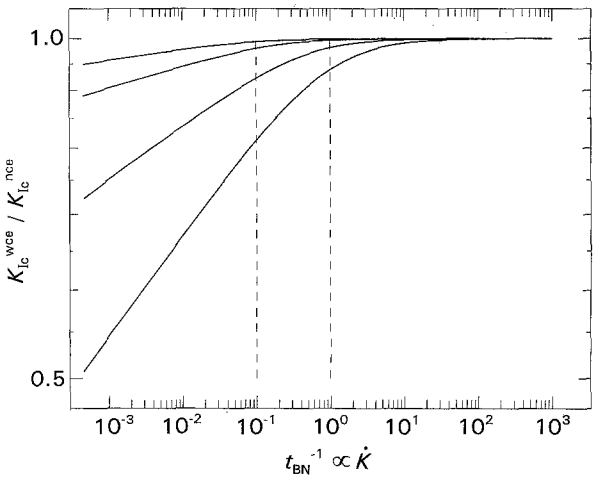

Figure 2 Influence of different values of the crack extension parameter, n, on fracture toughness in the LEFM theory: $n = 10$, 20, 50, 100, $B = 500$ MPa^{2}s. (– – –) The usual time range of fracture toughness experiments.

The structure of these equations is similar to the well-known loading-rate dependence of the bending strength. If one integrates the relation

$$\int_0^{t_f} \mathrm{d}t\, \sigma(t)^n = B\sigma_c^{n-2}\left[1 - \left(\frac{\sigma_B}{\sigma_c}\right)^{n-2}\right] \quad (13)$$

for $\sigma(t) = \dot{\sigma}t$ with σ_B the bending strength and σ_c the inert strength of the material, one obtains

$$\sigma_B^{n+1}\frac{1}{(n+1)\dot{\sigma}B} + \sigma_B^{n-2} = \sigma_c^{n-2} \quad (14)$$

which is exactly of the same type as Equation 9 – and the dependence of σ_B on low loading rates is equally $\dot{\sigma}^{1/(n+1)}$.

Therefore, one can conclude that at low temperatures, where the values of n and B are both high, the influence of subcritical crack growth is negligible for fracture toughness experiments. At high temperatures, however, where n is between 10 and 20 and B low, there is a strong influence of the loading rate on the fracture toughness, even in LEFM: the fracture toughness decreases with decreasing loading rate.

3. Fracture toughness dependence on loading rate due to the viscoelastic model

A viscoelastic model was proposed earlier [8] which described the fracture toughness by a model of springs and dashpots (Maxwell Elements). At the high loading rates, the springs are responsible for the K_{IC} value, at the low loading rates the dashpots are responsible. These limiting values can be experimentally determined by measurements at very high and very low loading rates. In a range between, both the springs and the dashpots can take up the strain and share the K-factor. Therefore, a higher K_{IC} value can be obtained. The viscoelastic K-factor is then

$$K_{visco}(t) = \frac{1}{N}\sum_i^N (K_{s_i}(t) + K_{d_i}(t)) \quad (15)$$

where N is the number of spring and dashpot elements. The viscoelastic K_{IC} (i.e. the specimen fails) is the K-factor, which the springs and dashpots can reach without exceeding their individual fracture toughness values, K_{IC_s} and K_{IC_d}, respectively

$$K_{s_i}(t) \leqslant K_{IC_s} \quad (16a)$$

$$K_{d_i}(t) \leqslant K_{IC_d} \quad (16b)$$

In this work, two improvements for the model proposed earlier [8] are suggested. First, the relaxation times of the dashpots $\tau_j = \eta_j/E$ are equally distributed in a logarithmic scale. This distribution gives the best results in the fit and is very simple

$$\log \tau_j = \log \tau_{max} + h\left(j - \frac{N}{2}\right) \quad j = 1 \ldots N \quad (17a)$$

$$\tau_j = \tau_{max} e^{h(j-N/2)} \quad (17b)$$

The parameter h defines the width of the distribution and N is the number of elements. Owing to limited computational resources, we constrained to 100 elements. τ_{max} and h are the two parameters which must be varied to obtain the best fit. τ_{max} is responsible for the maximum of the distribution of K_{IC}, h for the width and height of the maximum, respectively. Physically speaking, τ_{max} is a function of the viscosity of the second phase and h depends on the microstructure of the material (amount of glassy phase, grain size).

Second, the model can be improved by assuming that the fracture toughness, K_{IC_d}, of the dashpots is not constant, but shows an $\dot{F}^{1/(n+1)}$ dependence on the loading rate. This is a direct consequence of the results described in Section 2. A comparison of the fracture toughness in LEFM and in the viscoelastic model combined with the above assumptions is shown schematically in Fig. 3.

Contrary to the behaviour in the LEFM model, in the viscoelastic model both springs and dashpots can contribute to the K_{IC} factor and therefore in a certain range, a maximum of the fracture toughness can be obtained. This is the consequence of the possibility of crack extension promoted by the second phase, which enables the material to diminish the stress concentration at the crack tip and to display the stress into a "region of transformation".

Therefore, four parameters are required for the viscoelastic model:

(i) the limiting value, K_{IC_d}, for the dashpots, which can be obtained from measurements at very low loading rates;

(ii) the limiting value, K_{IC_s} for the springs, which can be obtained from measurements at very high loading rates;

(iii) τ_{max}, which describes the location of the maximum K_{IC} and is the mean time of relaxation from which the mean viscosity of the dashpots can be calculated;

(iv) h, which is responsible for the width of the maximum and represents the width of the distribution of the relaxation times of the dashpots.

τ_{max} and h result from fitting to the measured values of the fracture toughness at different loading rates.

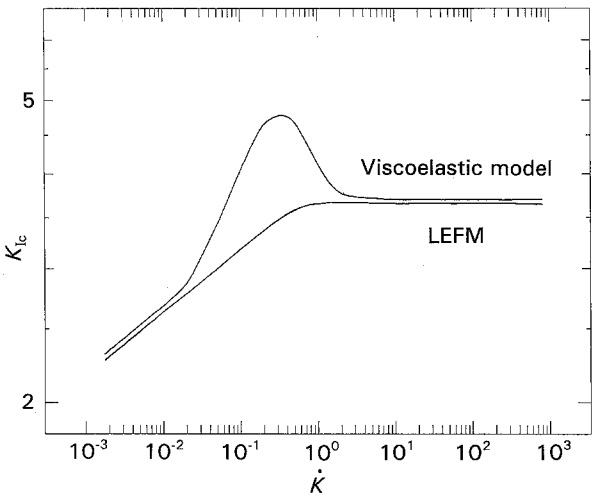

Figure 3 Comparison of fracture toughness in the viscoelastic model and in LEFM.

4. Discussion

Al_2O_3 with 3% glassy phase was used as a model material, because it shows a significant viscoelastic behaviour above 900 °C in the observed range of loading rates. The experiments were performed in air in a four-point bending device (fixed roller system [9]) with a span of 20/40 mm. The specimens were machined to the dimensions $3 \times 4 \times 45$ mm^3 according to DIN standard 51101.

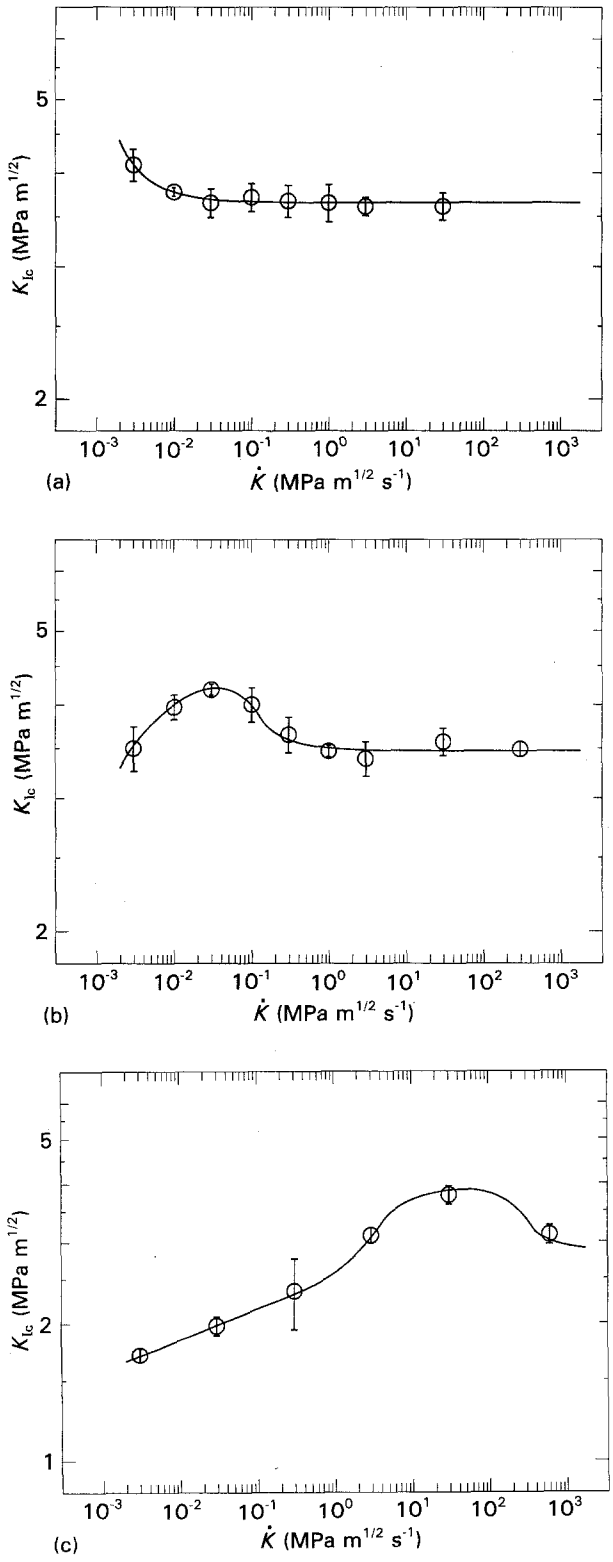

Figure 4 Experimental fracture toughness at different loading rates and calculated curve from the viscoelastic model at (a) 900 °C, (b) 1000 °C and (c) 1100 °C.

Fig. 4a and b shows the experimental values of K_{IC}, taken from earlier work [8] at 900 and 1000 °C. Fig. 4c shows the fracture toughness measured at 1100 °C: from this diagram one can clearly see the decrease of K_{IC} at low loading rates, as well as the shift of the maximum to higher loading rates. The occurrence of the maximum cannot be explained by LEFM, but by the viscoelastic model.

The lines in Fig. 4a–c are calculated with the viscoelastic model. They show a very good agreement with the experimental results (circles). For the fit, the subcritical crack extension parameter, n, was taken from corresponding four-point bending strength experiments. For 1100 °C, there is a large linear range in which the fracture toughness values decrease with decreasing loading rates. It was checked that the n values of the fracture toughness experiments and the n values taken from bending strength tests were identical within experimental error.

In earlier work [8], an exponential function was chosen for the functional dependence of the relaxation times. The shift of the fracture toughness with respect to the loading rate and the temperature was calculated using this relation. Fig. 5 is a three-dimensional diagram showing the dependence of the fracture toughness on both the loading rate and the temperature. Two characteristic features can be seen in this diagram. First, the maximum in the fracture toughness is shifted to higher loading rates for higher temperatures according to the exponential function for the dependence on the relaxation times and thus the respective viscosities. Second, the appearance of the maximum is higher and narrower at low temperatures. This is suggested by the fits as well as by the literature [2], where a lower loading rate could be experimentally realized. It may be a consequence of the fact that the relaxation time is shorter at higher temperatures. Hence the volume, to which the stress can be distributed, is larger. This is supported by measurements of the damage zone size, which increases faster than exponential for alumina in the range between 1000 and 1150 °C [10]. Thus many more grains of different

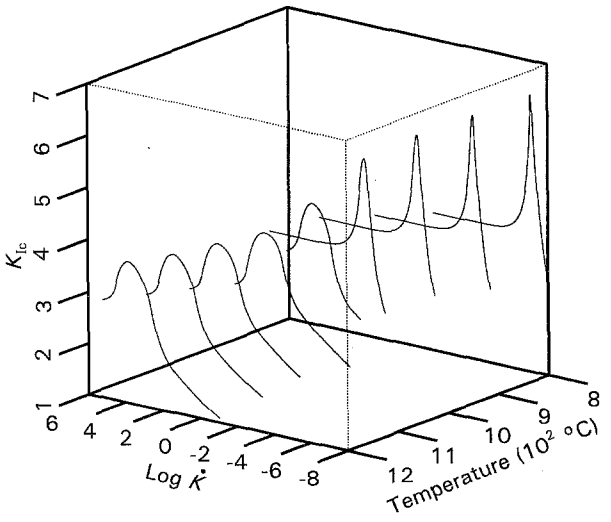

Figure 5 Dependence of fracture toughness on loading rate and temperature.

size and grain surfaces covered with glassy phase of different thickness are involved, resulting in a wider distribution of relaxation times.

5. Conclusion

In principle, it should be possible to calculate the maximum of fracture toughness (and the corresponding loading rate) from a knowledge of the viscosity of the second phase. Some questions, however, remain to be answered.

(i) Is there a geometry- (or loaded volume-) dependent factor? This is suggested by three-point bending tests, as the maximum is shifted to higher loading rates in these experiments [2] in comparison with the four-point bending tests. Moreover, K values at a higher level were observed in crack-resistance measurements [11], which could be explained by assuming that the loaded region is smaller in three-point bending than in four-point bending.

(ii) Is there an influence of the content of glassy phase?

(iii) Is the viscosity of the glassy phase in the bulk equal to the viscosity of thin films at the surface of hard grains? In any case diffusion of alumina of the grains into the glassy phase changes the viscosity significantly (by several orders of magnitude [12]).

In the meantime, it is proposed that fracture toughness tests of ceramics with glassy phase at high temperatures should be carried out at least three loading rates differing by several orders of magnitude. Fracture toughness can only be defined if those fracture toughness values are at the same level. Even in this case, the obtained fracture toughness cannot be taken as a material constant beyond the measured region of loading rates.

Acknowledgement

This work was supported by the Austrian Fonds zur Förderung der wissenschaftlichen Forschung, project P8990-PHY.

References

1. D. MUNZ, G. HIMSOLT and J. ESCHWEILER, "Fracture Mechanics Methods for Ceramic, Rocks and Concrete", ASTM *STP* **745** (American Society for Testing and Materials, Philadelphia, PA, 1981) pp. 69–84.
2. K. KROMP and R. F. PABST, *Metal Sci.* **3** (1981) 125.
3. G. POPP, PhD thesis, University of Stuttgart, FRG (1982).
4. J. WANG, P. A. WITHEY, C. B. PONTON and P. M. MARQUIS, *J. Mater. Sci. Lett.* **11** (1992) 1201.
5. European prestandard ENV 820-1.
6. DIN-standardization proposal 51110, parts 2 and 3.
7. Y. MURAKAMI, "Stress intensity factors handbook", Vol. I (Pergamon Press, Oxford 1987).
8. H. PETERLIK and K. KROMP, *J. Mater. Sci.*, **28** (1993) 4341.
9. C. RIEF and K. KROMP, *Int. J. High Technol. Ceram.* **4** (1988) 301.
10. R. L. TSAI and R. RAJ, *Acta Metall.* **30** (1982) 1043.
11. H. WIENINGER, K. KROMP and R. F. PABST, *J. Mater. Sci.* **22** (1987) 1352.
12. M. S. ASLANOVA, V. A. CHERNOV and L. F. KULAKOV, *Glass Ceram.* **31** (1974) 409.

Received 28 January
and accepted 24 November 1993